Complex patterns of abnormal heartbeats

Verena Schulte-Frohlinde,[1,2,*] Yosef Ashkenazy,[1,3] Ary L. Goldberger,[2] Plamen Ch. Ivanov,[1] Madalena Costa,[2] Adrian Morley-Davies,[4] H. Eugene Stanley,[1] and Leon Glass[5]

[1]*Center for Polymer Studies, Department of Physics, Boston University, Boston, Massachusetts 02215*

[2]*Cardiovascular Division, Harvard Medical School, Beth Israel Deaconess Medical Center, Boston, Massachusetts 02215*

[3]*Department of Earth, Atmospheric and Planetary Sciences, Massachusetts Institute of Technology, Cambridge, Massachusetts 02139*

[4]*Pilgrims's Hospital, Boston, Lincolnshire, PE 21 7QS, United Kingdom*

[5]*Department of Physiology, McGill University, Montreal, Quebec, Canada H3G IY6*

(Received 27 February 2002; published 4 September 2002)

Individuals having frequent abnormal heartbeats interspersed with normal heartbeats may be at an increased risk of sudden cardiac death. However, mechanistic understanding of such cardiac arrhythmias is limited. We present a visual and qualitative method to display statistical properties of abnormal heartbeats. We introduce dynamical ''heartprints'' which reveal characteristic patterns in long clinical records encompassing $\approx 10^5$ heartbeats and may provide information about underlying mechanisms. We test if these dynamics can be reproduced by model simulations in which abnormal heartbeats are generated (i) randomly, (ii) at a fixed time interval following a preceding normal heartbeat, or (iii) by an independent oscillator that may or may not interact with the normal heartbeat. We compare the results of these three models and test their limitations to comprehensively simulate the statistical features of selected clinical records. This work introduces methods that can be used to test mathematical models of arrhythmogenesis and to develop a new understanding of underlying electrophysiologic mechanisms of cardiac arrhythmia.

DOI: 10.1103/PhysRevE.66.031901 PACS number(s): 87.19.Hh, 89.20.−a, 89.75.−k, 87.10.+e

I. INTRODUCTION

The human heart displays an extraordinarily large range of complex rhythms, in both health and disease [1,2]. In the normal individual all beats arise from the upper chambers of the heart, the atria, in a rhythm set by a specialized pacemaker region called the sinus node. In some individuals, in addition to normal sinus beats, there are also abnormal beats originating from the ventricles, the lower chambers of the heart. The sporadic appearance of such ventricular ectopic beats is common and is not necessarily a cause for concern. However, an increased number of premature ventricular ectopic beats has been associated with an increased risk of sudden cardiac death [3]. This finding led cardiologists to hypothesize that medication to reduce the number of ventricular ectopic beats in patients who had suffered a heart attack could reduce the risk of sudden cardiac death. However, when clinical trials were carried out in patients treated with drugs that decrease the number of ventricular ectopic beats, the results surprisingly and dismayingly showed an increased rate of sudden death in the patients who received the medication compared to those who received a placebo [4]. There has been a subsequent diminution in interest in the analysis of the correlations between frequent ectopic beats and sudden death in the clinical literature.

The premise of the current work is that the dynamical patterns, not simply the number, of ventricular ectopic beats may contain important information concerning the underlying mechanisms of arrhythmia. Further, these mechanisms can be probed by appropriate quantitative analysis of lengthy (about 24 h) records, thereby possibly helping to identify individuals at high risk.

A variety of different quantitative approaches have been proposed to evaluate ventricular ectopic beats. These approaches include: counting the number of such beats in a given time interval, developing mathematical models of ectopic beats and fitting these to observed data for short time intervals [5–10]; and using computers to analyze data over several hours by developing novel methods to plot data to underscore mechanisms [11–13] or scaling properties [14–16]. Although these methods yield important information, they have not been useful in decoding the mechanisms of ectopic beats based on quantitative analysis of the dynamics.

To achieve this goal, we develop a method to analyze in detail the transient dynamics of ectopic beats in lengthy records, and we systematically study how different models can account for the observed dynamical patterns. The structure of the paper is as follows. In Sec. II we introduce the basic terminology concerning the beat intervals in cardiac arrhythmia. In Sec. III we introduce four clinical 24 h records which were selected to illustrate different patterns of complex arrhythmia. We do this by introducing a procedure we call the dynamical ''heartprint''—a graphical montage of histograms useful in identifying different properties of the arrhythmia and their changes. In Secs. IV to VII we present four simple models to study the dynamics of ventricular ectopic beats. We try to understand the dynamics in ''real world'' clinical data in terms of these models. A discussion follows in Sec. VIII. A preliminary account of some aspects of this work has recently appeared in Ref. [17].

II. TERMINOLOGY CONCERNING BEAT INTERVALS IN CARDIAC ARRHYTHMIA

Figure 1 shows an excerpt of an electrocardiogram of a patient with normal sinus beats (*S*) as well as abnormal ven-

*Electronic address: frohlind@argento.bu.edu

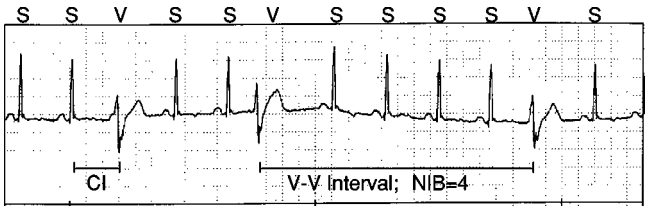

FIG. 1. Electrocardiogram over a time interval 6.6 s of a patient with heart failure (Record 3 of Fig. 2). Sinus (*S*) and ventricular (*V*) beats differ in shape. The ventricular ectopic beats each block the appearance of a sinus beat but do not alter the sinus rhythm otherwise. Examples for a coupling interval (CI), and a *V*-*V* interval with the corresponding number of intervening sinus beats (NIB) are indicated.

,tricular ectopic beats (V), which are distinguishable by their characteristic morphologies. After each heartbeat, regardless of its origin, there is a period θ, called the refractory time, during which no other heartbeat can be expressed. Thus, if a ventricular beat (depolarization) falls inside the refractory time θ after a sinus beat, that ventricular beat is not expressed; it is concealed (blocked). However, if the ventricular beat falls outside the refractory period, then it is expressed and the following sinus beat is usually blocked. In some cases, for example, if a ventricular ectopic beat falls during a relatively long sinus beat interval, the following sinus beat may not be blocked, in this case the *V*-beat is said to be *interpolated*. Although it is not evident from the short record in Fig. 1, the sinus rate normally fluctuates considerably during the course of the day [18]. These fluctuations reflect the operation of a number of different mechanisms so that the cardiac output is matched to physiological activity [19]. The control is exerted via autonomic nerve activity directly to the heart as well as via circulating hormones. Factors that modulate the heart rate can also affect the mechanisms underlying the ectopic beat formation [20].

Ventricular ectopic beats may arise from several different electrophysiologic mechanisms [1,2] including the following. In *reentry*, the excitation wave following a normal sinus impulse travels through a loop of ventricular muscle to reexcite the heart tissue, usually at a fixed delay after the normal sinus beat. For example, a reentrant pathway could be formed as a circuit of viable tissue in an area of a scar caused by a previous myocardial infarction (''heart attack''). In *triggered activity*, the action potential of the excitation wave following a normal beat triggers early or late ventricular afterdepolarizations. Both types of triggered arrhythmias can lead to either a single beat, or a sequence of impulses beginning at a fixed time interval following the sinus beat. The third basic mechanism for ventricular ectopic beats is an *independent spontaneous pacemaker* in the ventricles which competes with the normal sinus rhythm. This class of arrhythmias is called parasystole. The ventricular pacemaker may have a fixed frequency, or it may be reset by the sinus pacemaker [6,8]. Independent of the mechanism, a given ventricular beat will only be observed on the electrocardiogram if it falls outside of the refractory period induced by the preceding beat.

The characterization of complex ventricular rhythms leads to the definition of a number of terms, illustrated in Fig. 1. The sinus beat interval, T_S, is the time between successive sinus beats and the *V*-*V* interval is the time between successive ventricular beats. The coupling interval, CI, is the time from an ectopic beat to the previous sinus beat. The number of intervening sinus beats, NIB, between each two successive ectopic beats is an integer that may reveal distinctive statistical properties. (If the first of the two ectopic beats is interpolated we do not include the first normal beat into the NIB value unless otherwise stated.)

Finally, for a given time period, the number of expressed ectopic beats, n_V, divided by the total number of sinus beats, expressed and concealed, N, gives the fraction n_V/N of beats that are ectopic. One of the features that makes the study of ventricular ectopic beats so challenging is that all of these parameters may change during the course of the day. Although the precise mechanisms that lead to the changes may differ from person to person, in many cases there appears to be a strong correlation between these changes and the sinus cycle time. Consequently, we have developed some techniques for presenting clinical data, by plotting each of the above quantities as a function of the sinus cycle time.

III. HEARTPRINT PRESENTATIONS OF DATA

We plot the parameters describing complex arrhythmia in the form of what we call dynamical ''heartprints'' (see Fig. 2). The heartprint is a way to represent dependences between the sinus interval and (i) the ectopic interval (*V*-*V*), (ii) the number of intervening sinus beats between ectopic beats (NIB), and (iii) the CI. We represent these dependences in gray scale plots (where the darker shading represents more events) [21]. The ordinate in each case represents the sinus beat interval. The abscissa represents the *V*-*V* interval, the NIB, and the CI, respectively. The histogram of sinus beat intervals is shown at the left of the figure, and the histograms of the *V*-*V* intervals, the NIB, and the CI are shown above the gray scale plots. Thus each heartprint contains seven panels.

In Fig. 2 we show the heartprints for 24 h recordings of four different patients with life-threatening heart disease and frequent ventricular ectopic beats (>5000 beats/24 h). Three cases are associated with congestive heart failure [(a), (c), and (d)], whereas Record 2 in (b) is from a patient at high risk of sudden cardiac death whose record also shows prolonged runs of consecutive ventricular ectopic beats (ventricular tachycardia). These four patients represent notable classes of patterns we observed by inspection of recordings from ≈ 50 patients with heart failure. However, they are not intended to represent the broad range of conditions associated with premature ventricular beats. We briefly describe the heartprint of each record, and then discuss the differences between them.

Record 1. The heartprint of Record 1 is shown in Fig. 2(a). The gray scale plot of the *V*-*V* intervals as a function of the sinus beat intervals shows a diagonal line structure consisting of linearly increasing lines implying that many *V*-*V* intervals coexist for each sinus beat interval. Further, the *V*-*V* intervals increase linearly with the sinus beat interval.

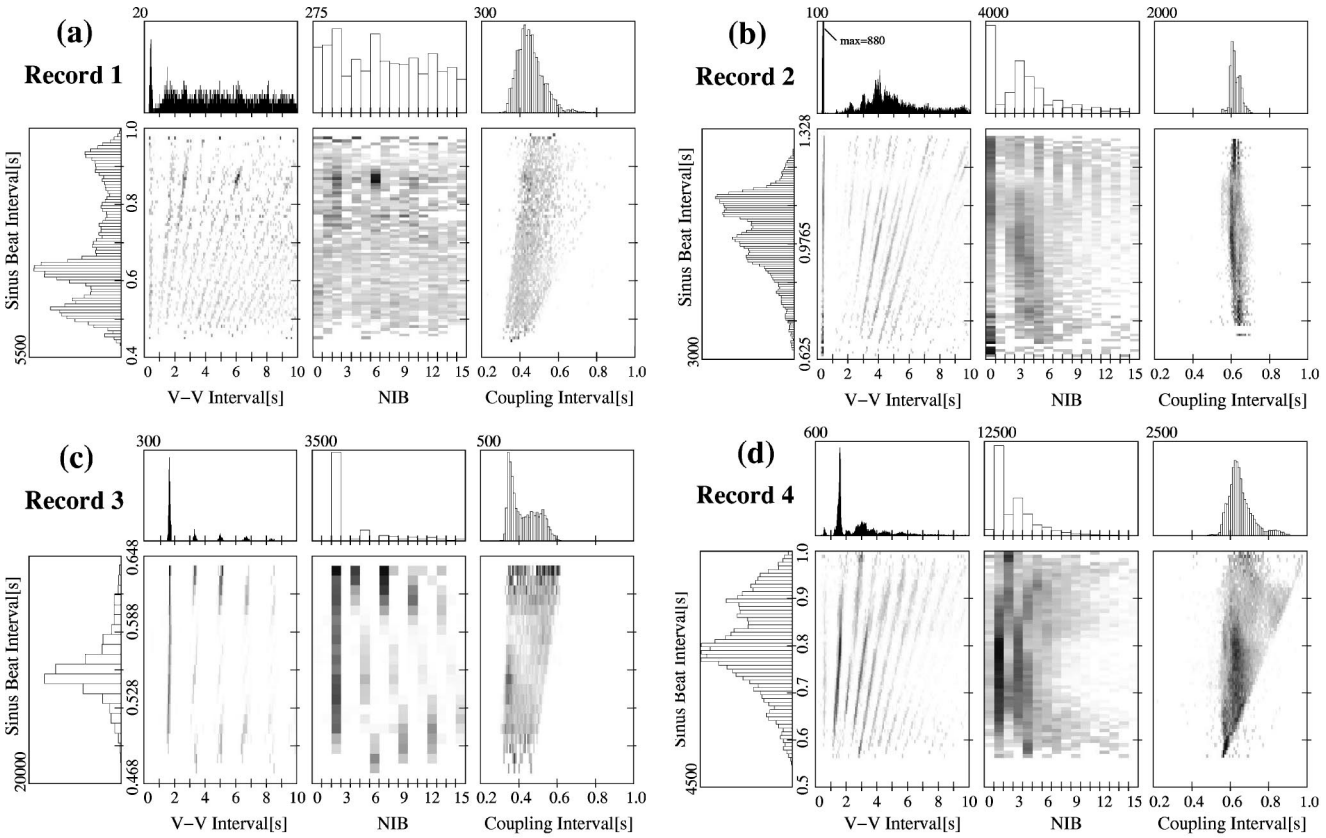

FIG. 2. Heartprints for ~24 h clinical records (a) Record 1, (b) Record 2, (c) Record 3, and (d) Record 4. See text for a detailed explanation.

This structure is a common feature of such records and may arise from the restriction of the occurrence of ectopic beats to the time interval following the refractory time of the preceding sinus beat. If the variability of the coupling intervals is even more restricted, the line structure will be more pronounced. However, the histograms of the *V-V* intervals and the NIB show little structure. The ectopic ventricular beats predominantly occur with a coupling interval of 0.35–0.55 s. This record shows much less structure than the following records.

Record 2. The heartprint of Record 2 [Fig. 2(b)] is very different from that of Record 1. The histogram of the *V-V* intervals shows a narrow peak at approximately 0.38–0.40 s and then several broad peaks at larger *V-V* intervals. The narrow peak at the 0.38–0.40 s is due to ventricular *couplets*, in which there are two consecutive ventricular ectopic beats, or to longer sequences of ventricular ectopic beats without intervening sinus beats. The gray scale plot of the *V-V* intervals as a function of the sinus beat intervals again shows a diagonal line structure. At some sinus rates there are two parallel diagonal lines separated by about 0.38–0.40 s which are associated with the frequent couplets. The coupling interval is sharply peaked in the range of 0.6–0.7 s. In contrast to the preceding example, the NIB show some interesting structure. For sinus beat intervals less than 1.0 s, low NIB values (2–5) predominate, whereas for sinus beat intervals greater than 1.15 s the NIBs take only odd values, mainly 5, 7, and 9. (For $T_S > 1.1$ s, the single ectopic beats that are not part of a couplet, are all interpolated. As mentioned earlier, the normal beat immediately following an interpolated one is not included in the NIB count. Thus, the NIB pattern in Fig. 2(b) is not changed by the appearance of the interpolated beats.)

Record 3. The sinus beat intervals in the heartprint of Record 3 [Fig. 2(c)] are constrained in the narrow range of $T_S = 0.55 \pm 0.10$ s. A prominent feature here is that the histogram of the *V-V* intervals consists of equidistant peaks with a spacing of ≈ 1.6 s. The gray scale plot of the *V-V* intervals now shows a vertical line structure reflecting the observation that the *V-V* intervals are integer multiples of a common divisor independent of the sinus beat interval. This suggests that at the origin of the abnormal beats might be a periodic pacemaker with a period $T_V \approx 1.6$ s [17]. In this record there is order in the structure of the NIB that we will discuss in detail later. The coupling intervals take all values in the interval between ≈ 0.33 s and the next sinus beat.

Record 4. The heartprint of Record 4 [Fig. 2(d)] has similarities to Record 3 in that we see distinct values for the NIBs. However, the peaks in the *V-V* interval histogram are not equidistant. In fact, the diagonal line structure of the *V-V* intervals is a feature we saw in Records 1 and 2. Also, the coupling interval histogram is peaked but the gray scale plot of the coupling interval as a function of sinus beat interval shows that the ectopic beats can occur in the time interval between ≈ 0.55 s and the next sinus beat. (No interpolated beats are present in this record.)

We now briefly describe the most apparent differences

among the four records and their potential relevance to the underlying mechanisms. The plots of the coupling interval as a function of the sinus beat intervals show different structures in the different records. In Record 2, the coupling interval is approximately the same for all sinus rates whereas the other records show much more variability. The refractory time of the heart following a sinus beat must be shorter than the shortest coupling interval. The longest coupling interval must be shorter than the sinus cycle time. Therefore, if all possible coupling intervals occur for any given sinus rate, there will be an almost triangular (or quadrilateral) structure in the CI gray scale plots as was observed in Records 3 and 4, and the lower bound of the coupling interval may give information about the refractory time and its dependence on the sinus cycle length. In the case of fixed coupling intervals the refractory time may be estimated from the occurrence of interpolated beats. The shortest interval occurring between a *V* beat and a following interpolated sinus beat gives an upper limit for the refractory time of the heart tissue. For Record 2 we find $\theta \approx 0.57-0.6$ s.

Since a fixed coupling interval means that the ectopic beat occurs at a fixed time interval after a sinus beat, fixed coupling intervals have been taken to imply either a reentrant mechanism or a triggered mechanism. In contrast, if the coupling intervals vary over a broad range for any given sinus cycle length, then the ectopic mechanism would appear to be independent of the preceding sinus cycle. This could occur if there were an independent ectopic pacemaker or if the ectopic beats were generated randomly in time. In Record 1 the coupling intervals appear to be quite broad and featureless, suggesting a random mechanism, whereas the fixed time intervals between the *V*-*V* beats in Record 3 suggest an independent pacemaker in this record.

The heartprints also show differences in the patterns of the NIB values. It is remarkable that these records show areas where the NIB values assume only odd values (as occurs in Record 2), or assume one of the values 2,5,8,11, . . . (as occurs in Record 3). Although previous workers have examined mechanisms that can give rise to this sort of rhythms [5–13], the systematic study of arrhythmia over long periods of time is only made possible by computerized analysis of extended records. A mechanism that might appear valid over a short interval might be inconsistent with the data in an extended record.

Another way to compare the patterns of ectopy in different records is to plot the fraction n_V/N of ventricular ectopic beats as a function of the sinus beat interval (Fig. 3), where n_V is the number of expressed *V* beats and *N* is the total number of normal beats, expressed and concealed. The solid points represent the data, whereas the open symbols and the superimposed lines represent the behavior of models that are presented below. Once again, there are distinct differences among the records. The above discussion suggests theoretical models that might be appropriate for the analysis of the complex ectopy. We present three different classes of models whose basic features are intended to capture fundamental physiologic mechanisms including parasystole and reentry as described in Sec. II.

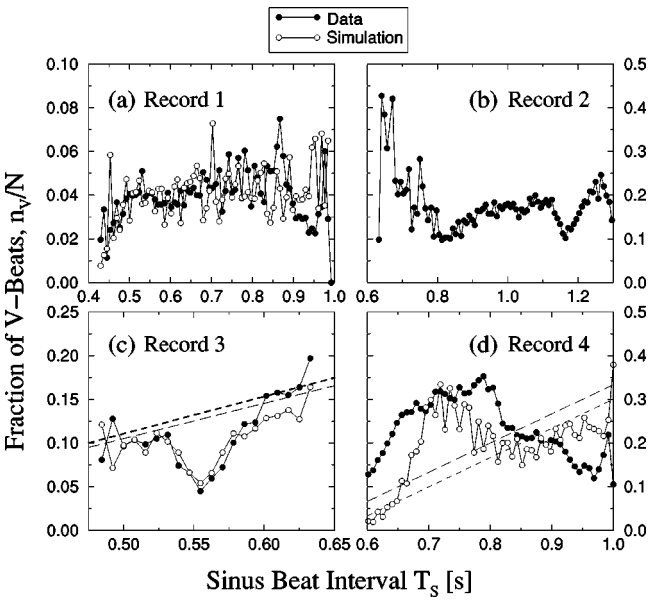

FIG. 3. Fraction n_V/N of appearing *V* beats, where n_V is the number of appearing *V* beats, and *N* the sum of appearing and concealed normal beats, versus sinus beat intervals. (a) Record 1 together with the simulation from Fig. 7. (b) Record 2; (c) Record 3, and the result of a corresponding simulation of modulated parasystole (Fig. 11). The lines are given by Eq. (7) for two different periods of the independent ventricular pacemaker $T_V = 1.67$ s and $T_V = 1.76$ s, and the refractory time linearly dependent on the sinus beat interval $\theta = 0.29T_S + 0.17$ s. Note that the curves for the data and simulation with weak coupling deviate from the lines at $T_S = 0.55$ s. (d) Record 4, and a simulation of strongly modulated parasystole (Fig. 12). The line is again given by Eq. (7) with $T_V = 1.5$ s and $\theta = 0.5$ s and $\theta = 0.55$ s, respectively.

IV. MODEL 1: RANDOM VENTRICULAR ECTOPIC BEATS

Perhaps the simplest assumption concerning the ectopic beats is that they occur randomly in time. This model is useful because it serves as a baseline for comparing heartprints, since the only way in which this model generates patterns is through the refractory times of the sinus and ectopic beats. We simulate [22] a record in which the probability for an ectopic beat is $p_0 = 0.5$/s [23]. The distribution of the *V*-*V* intervals of such randomly appearing ectopic *V* beats is of the form

$$p(t) = p_0 \exp(-p_0 t). \tag{1}$$

However, since after each heartbeat the heart is refractory for a time interval θ, the appearance of the ectopic *V* beats is limited to time intervals when the heart is not refractory. This generates the diagonal line structure in the gray scale plot of the *V*-*V* intervals [Model 1 in Fig. 4(a)]. For T_S fixed and for small $\Delta t = T_S - \theta > 0$, the histograms of *V*-*V* intervals consist of a series of sharp peaks with a spacing of approximately T_S. Using the Poisson distribution we find that the integrated density in the peak centered at $(n+1)T_S$ is given by

$$(1-p_0\Delta t)^n p_0 \Delta t. \tag{2}$$

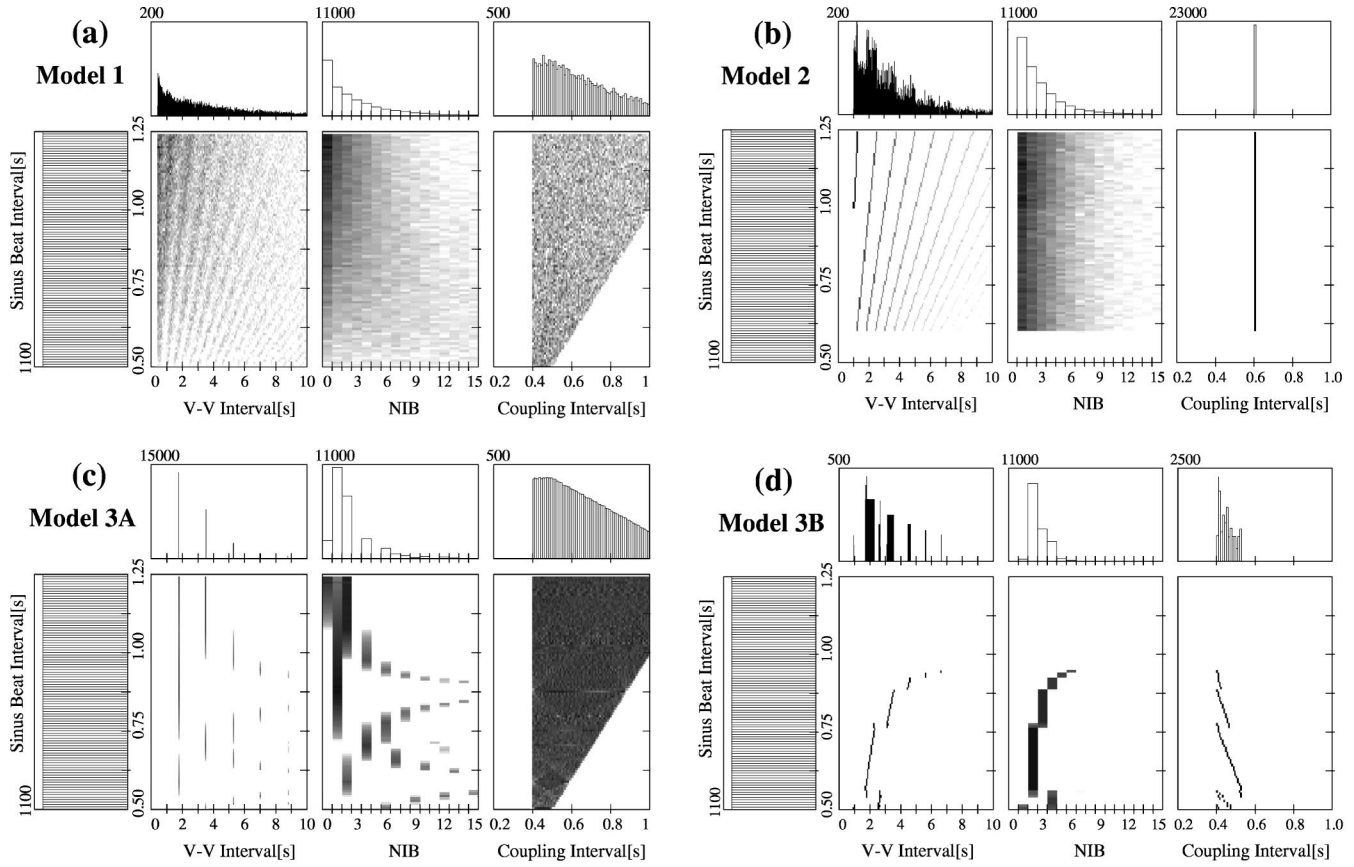

FIG. 4. The heartprint for the basic models [22]. (a) Model 1, random distribution of ventricular beats; (b) Model 2, fixed delay; (c) Model 3A, independent pacemaker; and (d) Model 3B, coupled pacemaker. See text for a detailed explanation.

The actual distribution of the V-V intervals for fixed T_S lies between these two limiting cases: Eq. (1) for zero refractory time and Eq. (2) for maximal refractory time.

We choose $\theta = 0.4$ s in all simulations of the basic models since this is a value typically found in clinical records. Figure 5(a) shows schematically a beat sequence resulting from such a model. The heartprint generated with this model is shown in Fig. 4(a). For a larger value of the refractory time θ the diagonal line structure in the gray scale plot on the V-V intervals is more pronounced, approaching the discrete case for $\theta \sim T_S$.

In the plots of coupling intervals as a function of the sinus beat intervals, the density distribution is uniform as expected for randomly distributed V beats.

To find an expression for the fraction of V beats as a function of the sinus beat intervals we start with the probability to find a V beat in a time period T_S, which is $p_0 T_S = 0.5 T_S$. The probability for the V beat to fall outside of the refractory time of a normal beat is given by $(T_S - \theta)/T_S$. The fraction of V beats is then given by the product of these two terms,

$$\frac{n_V}{N} = p_0(T_S - \theta) = 0.5(T_S - 0.4). \tag{3}$$

The line given by Eq. (3) is plotted in Fig. 6(a). It overestimates the number of ectopic beats because the randomly

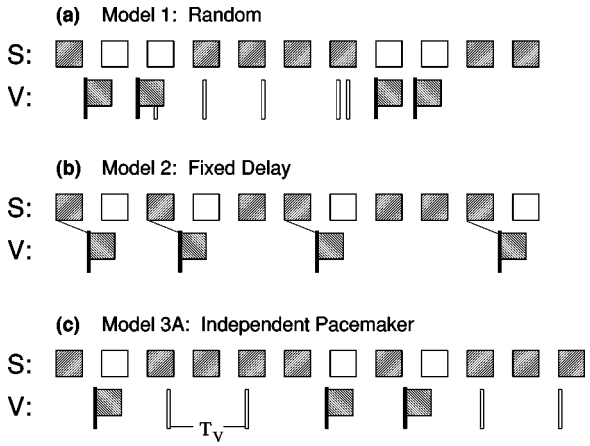

FIG. 5. Schematic illustration of the sequence of normal beats (upper boxes) and ectopic beats (black bars with lower boxes) for the three basic electrophysiologic models for the generation of ventricular ectopy. Expressed beats are shaded, blocked beats are empty (normal beats) or have no box (V beats). The sinus beat interval is $T_S = 0.7$, the refractory time (boxes) is $\theta = 0.4$ (arbitrary units). (a) Model 1, random V-beat distribution (Model 1); (b) Model 2, fixed delay with a coupling interval CI = 0.5 (Model 2); and (c) Model 3A, independent pacemaker (parasystole) with the period $T_V = 1.2$.

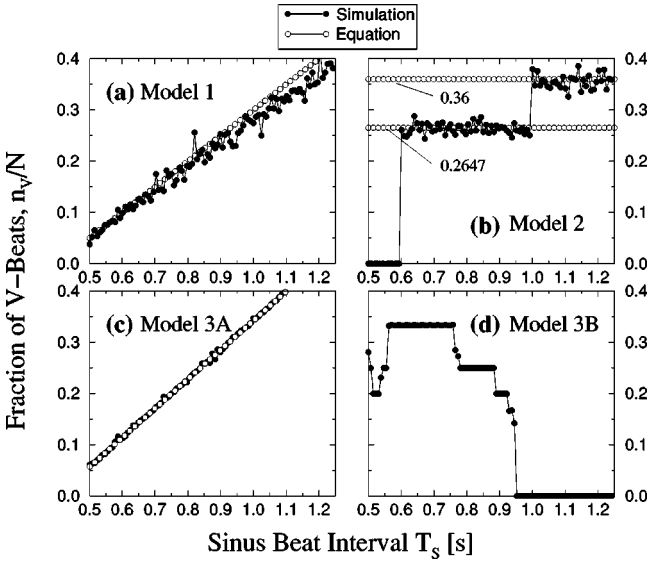

FIG. 6. Fraction n_V/N of manifest *V* beats plotted against sinus beat intervals for model simulations (Fig. 3). (a) Model 1 (random distribution of *V* beats), and Eq. (3). (b) Model 2 (*V* beats randomly generated by a preceding normal beat with a fixed coupling interval) and Eqs. (4) and (5). (c) Model 3A (independent pacemaker with the period $T_V \approx 1.5$ s) and Eq. (7). (d) Model 3B, the same as (c) but with the coupling shown in Fig. 10 between the pacemakers. The coupling changes the curve significantly.

timed *V* beats may block each other due to the refractoriness of the heart tissue. This reduces the probability p_0 and therefore the slope in Fig. 6(a).

The assumption of random occurrence of ectopic beats does not fully correspond to the dynamics observed in any of the records. Although the data in Record 1 have some similarity to what is expected with randomly occurring ventricular beats, this record is better discussed in the context of the next model.

V. MODEL 2: *V* BEATS WITH FIXED COUPLING INTERVAL—REENTRY AND TRIGGERED ACTIVITY

In Record 2, all of the ectopic beats occur at a fixed coupling interval following the preceding sinus beat. A simple model that could display such dynamics is the one based on a reentrant mechanism or a triggering mechanism. After each expressed normal beat we generate a *V* beat with probability *p*. If a *V* beat appears, it occurs at a fixed coupling interval CI after the normal beat as shown in Fig. 5(b). In a simulation [22] of the model, we choose CI$=0.6$ s, and $p=0.36$. The resulting heartprint is shown in Fig. 4(b) (Model 2). *V* beat activity starts when $T_S >$ CI. The fixed delay leads to a straight line at CI$=0.6$ s in the gray scale plot of the coupling intervals. The distribution of the number of intervening beats (NIB) is independent of the sinus beat intervals since the probability for the appearance of a *V* beat does not change with T_S. Consequently, the probability that the NIB value is equal to $n+1$ is given by $(1-p)^n p$. In Fig. 5(b) we see that, for NIB$=n$, the *V*-*V* interval is $(n+1)T_S$, and this is reflected in the gray scale plot for the *V*-*V* intervals in Fig. 4(b). The smallest *V*-*V* interval is therefore equal to $2T_S = 1.2$ s since every *V* beat conceals the next normal beat and only the next normal beat can generate another *V* beat. For T_S larger than $CI+\theta \approx 1.1$ s all *V* beats are interpolated, i.e., the following normal beats are not concealed and may generate a *V* beat on their own. In this case, the smallest *V*-*V* distance is equal to T_S. This is the only exception where the NIB values following an interpolated *V* beat do include the nonconcealed normal beat because otherwise we may generate NIB$=0$, which is not possible in the mechanism.

To calculate the fraction of *V* beats we must consider that only expressed normal beats generate *V* beats, and subtract the number of concealed normal beats (=number of expressed *V* beats n_V) from the total number of normal beats *N*. Hence $n_V=(N-n_V)p$, so

$$\frac{n_V}{N} = \frac{p}{1+p}. \tag{4}$$

For $p=0.36$, $n_V/N=0.2647$. In Fig. 6(b), we plot n_V/N and compare with the simulated curve. For T_S larger than $CI+\theta=1.0$ s no normal beats are concealed, such that all beats contribute to the generation of *V* beats, and we find

$$\frac{n_V}{N} = p \quad \text{for } T_S > 1.0 \text{ s}. \tag{5}$$

Comparison with Record 1. The rhythm displayed in Record 1 in Fig. 2(a) has features in common with Model 1 in Fig. 4(a), as well as with Model 2 in Fig. 4(b). The *V*-*V* intervals and the coupling intervals are more restricted than in Model 1 but less than in Model 2. This is not due to a large refractory time θ, since the gray scale plot of the coupling intervals gives 0.3–0.4 s as upper limits for the refractory time. Therefore, we simulate Record 1 by assuming a mechanism similar to the fixed coupling interval mechanism of Model 2 in Fig. 4(b) where each expressed normal beat generates with probability *p* a *V* beat. Instead of fixed cou-

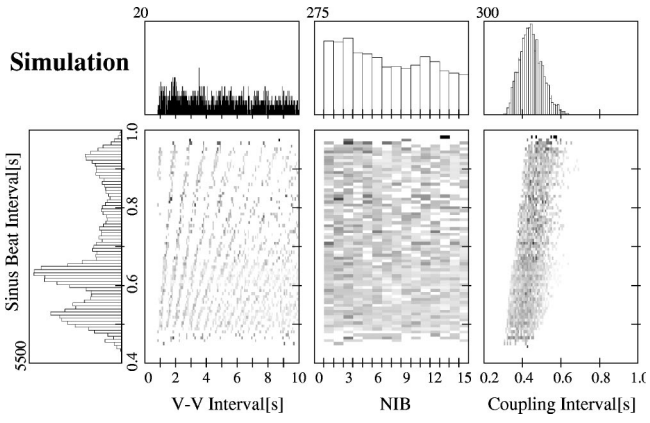

FIG. 7. Simulation for Record 1 [Fig. 2(a)] in which each normal beat generates a *V* beat with probability $p=0.045$, similar to Fig. 4(b) but the coupling intervals are drawn from Gaussian distributed noise. The center of the Gaussian is linearly dependent on the sinus beat intervals: $0.29+0.21T_S$. We use the sinus beat intervals of Record 1 in the simulation.

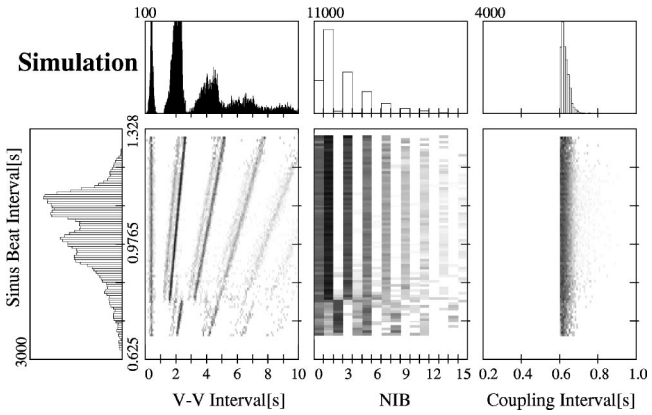

FIG. 8. Simulation of the reentry mechanism with $\theta_{\mathrm{Loop}}=1.6$ s and a fixed travel time $\tau=0.6$ s plus Gaussian distributed noise ($\sigma=0.03$ s), and refractory time $\theta=0.6$ s. The concealed bigeminy (NIB=1,3,5,7, . . .) is reproduced but in the data NIB $=1$ does not appear. The couplets were also simulated by randomly deciding with probability 1/2 if a *V* beat should follow a *V* beat. Again, the sinus beat intervals from the data were used.

pling intervals we use Gaussian-distributed coupling intervals to incorporate the randomness from Model 1. The center of the Gaussian distributed coupling intervals increases linearly with T_S. It is known that the refractory time can increase with increasing sinus beat intervals. For the simulation, we also use the actual sinus beat intervals from the data. The heartprint in Fig. 7 shows the result. The features of Record 1 can almost entirely be reproduced. We do not generate the narrow peak at very small *V*-*V* intervals since they result from ventricular couplets which we do not include in this simulation.

Comparison with Record 2. Since there is a fixed coupling interval in Record 2 [Fig. 2(b)], this record is a candidate for simulation by a model for reentry or triggered activity. The heartprint of Record 2 also shows peaks in the NIBs. These cannot be reproduced with the basic Model 2. We have attempted to simulate the data in this record by developing a model for reentry in which the conduction through the reentrant pathway depends on prior activity. This physiological property can be described with a refractory time $\theta_{\mathrm{Loop}}\neq\theta$ for the reentry pathway [10,13]. The travel time through the reentry loop (which gives the coupling interval CI if a ventricular beat is generated) may depend on the recovery time that has elapsed since the previous travel through the loop. The functional form for this dependence could be a decaying exponential [24]. The more the time that has passed since the last travel through the loop, the faster the travel will be. Eventually it may be so fast that the excitation wave meets refractory tissue after traveling through the loop such that no *V* beat is generated. This model is described in the Appendix.

In Record 2, however, the coupling intervals are almost fixed. We therefore chose for the travel time a fixed number plus some fluctuations. If the travel time equals the refractory time these little fluctuations will conceal some ventricular beats. The refractory time of the loop is chosen such that the NIBs take only odd numbers as shown in the simulation for Record 2 in Fig. 8.

In the data, however, mainly NIB=5,7,9 . . . are present for $T_S>1$ s. The lower sinus beat interval part in Fig. 2(b) can be generated by setting the refractory time of the loop large enough to reach NIB$\approx$3,4,5, i.e., $\theta_{\mathrm{Loop}}\approx 5T_S$, and adding a lot of noise.

Thus, the generation of both, the low and the high T_S patterns present in Fig. 2(b), seems impossible with the current model with fixed parameter settings. The double lines in Fig. 2(b) are reproduced in Fig. 8 by randomly allowing ventricular beats to be followed by other ventricular beats.

VI. MODEL 3A: INDEPENDENT PACEMAKERS—PURE PARASYSTOLE

We now assume that an independent pacemaker with period T_V is the source of the ventricular beats as shown in the cartoon in Fig. 5(c). This mechanism is called *pure parasystole* [6,9] and Fig. 5(c) displays a schematic plot of a beat sequence. The heartprint resulting from a simulation [22] of this model with $T_V=1.75$ s and $\theta=0.4$ s is shown as Model 3A in Fig. 4(c). The histogram of the *V*-*V* intervals consists of equidistant peaks which are separated by the period T_V. The fact that there is more than one peak is due to the refractory time which conceals some of the abnormal beats and leads to *V*-*V* intervals that are integer multiples of T_V. The corresponding gray scale plot shows lines that are not tilted. We also see that at most three different *V*-*V* intervals or NIB values are found for any given sinus beat interval.

A mathematical description [6,9] of such a model introduces the phase ϕ_i of the ith *V* beat in the sinus cycle, i.e., the coupling interval divided by T_S. Successive values of ϕ_i are determined by iterating the difference equation (circle map),

$$\phi_{i+1}=(\phi_i+T_V/T_S) \mod 1, \tag{6}$$

where a *V* beat is expressed if $\phi_{i+1}>\theta/T_S$. This equation depends on only two parameters, the ratio of the two periods T_V/T_S, and the ratio of the refractory time to the sinus period θ/T_S. For an irrational ratio T_V/T_S (incommensurate periods) the *V* beats will, for sufficiently long times, be equally distributed in the sinus cycle, i.e., the phases ϕ_i will take all values between θ and 1 with equal probability. The NIB sequence then has the following properties [6,9]: (i) there are at most three different values for the NIB; (ii) the sum of the two smaller NIBs is the largest NIB minus one; and (iii) only one of the NIB values is odd. The θ/T_S, T_V/T_S-parameter space can be completely partitioned into regions of these triplets as in Fig. 9. If the ratio of the periods of the two pacemakers is close to an integer n, the sequence of NIBs contains long sequences of $n-1$ interrupted occasionally by two large numbers. For $n=2$ this yields a pattern called bigeminy (NIB=1), since every second beat can be a *V* beat; for $n=3$ the rhythm is called trigeminy.

The uniform distribution of the phases of the *V* beats allows us to derive the fraction of *V* beats which are observed at a particular T_S. The probability for a *V* beat to be generated in a time period T_S is given by T_S/T_V. Of these a

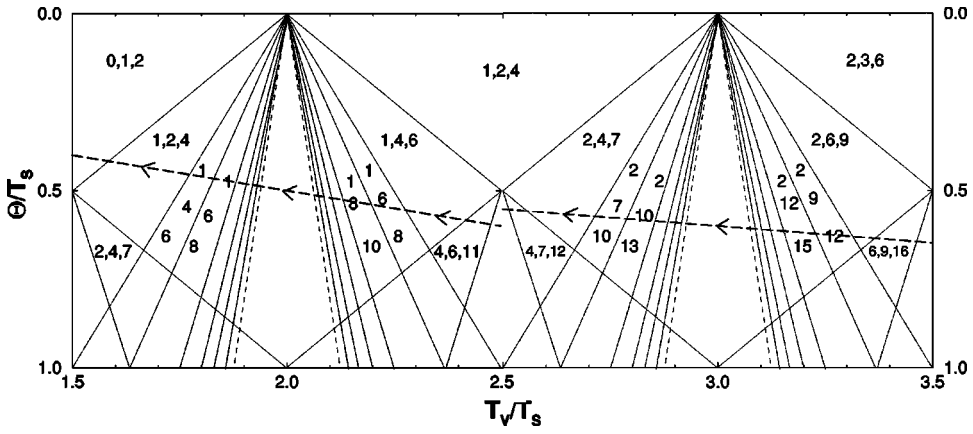

FIG. 9. Parameter plots of the NIB triplets in parasystole as adapted from Ref. [9]. For each set of parameters θ/T_S, T_V/T_S three NIB values make up the NIB sequence. The organization of the sequence varies within the region of any given triplet. The dashed lines indicate increasingly narrow regions with triplets made up from T_V/T_S-1, and two large numbers. The dashed arrows on the left-hand side show the region relevant for Record 4, and the dashed arrow on the right-hand side for Record 3.

fraction of $(T_S-\theta)/T_S$ occurs outside the refractory period and is observed. The ratio of the number of the observed V beats n_V to the total number of normal beats (observed and concealed) N is then [25]

$$\frac{n_V}{N}=\frac{T_S}{T_V}\frac{T_S-\theta}{T_S}. \tag{7}$$

Perturbation of the timing of the V beats by noise does not affect this distribution since it does not affect the uniform distribution of the phases. But any coupling between the two oscillators will change this distribution as well as the distribution of the coupling intervals in dependence on the sinus beat intervals [25].

Comparison with Record 3. Comparison between Model 3A in Fig. 4(c) and Record 3 in Fig. 2(c) immediately suggests that the origin of the V beats in Record 3 may be an independent (parasystolic) pacemaker. In the V-V interval histogram Fig. 2(c), we see, however, that the peaks have some broadness. A closer look at the corresponding gray scale plot reveals a substructure in the vertical lines. This substructure consists of parts of the diagonal lines familiar from Fig. 2(a). It seems that the present mechanism selects those points out of underlying diagonal lines which equal a multiple of the period T_V plus some noise. The noise leads to the broadness of the vertical lines.

As mentioned above, in the case of parasystole we expect the occurrence of only three different NIBs, whose values depend on the sinus interval. But, we clearly find more than three NIB values for each sinus beat interval. Comparison with the theoretical values for the NIB in Fig. 9 ($<2.5T_V/T_S<3.5, \theta/T_S\approx 0.6$) shows that the NIB values at the edges ($T_S<0.53$ s and $T_S>0.57$ s) are reproduced. In addition to the triplet we find the NIBs from neighboring sinus beat intervals. In the center, however, we find the NIB sequence 2,5,8,11 instead of just 2. These discrepancies from pure parasystole can be accounted for by noise affecting the periods of the two pacemakers [17].

Another important feature of a system of two uncoupled oscillators is the uniform distribution of the phase shift between the two oscillators which corresponds to the uniform distribution in the gray scale plot of the coupling intervals of Model 3A in Fig. 4(c). For Record 3, the entire allowed triangular space is filled but the varying gray scale implies a nonuniform distribution of the probability. Some coupling intervals are preferred compared to others. In addition, we compare the fraction of V beats in the data [Fig. 3(c)] and in the simple model for pure parasystole [Fig 6(c)]. We find that close to the ratio $T_V/T_S=3$ many V beats predicted by the

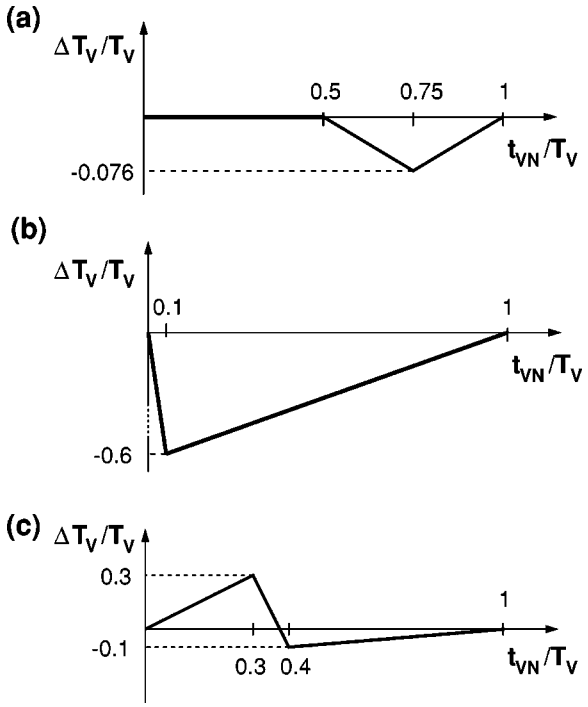

FIG. 10. Coupling mechanism between two pacemakers. The change ΔT_V of the period of the V oscillator as a function of the ratio of the time t_{VN} between the last V beat and a normal beat, and T_V. The coupling shortens the intrinsic T_{V_0} to the apparent T_V. (a) shows the weak coupling used to simulate Record 3 in Fig. 11. (b) shows the strong coupling used to simulate the model in Fig. 4(d). (c) shows the coupling used to simulate Record 4 in Fig. 12.

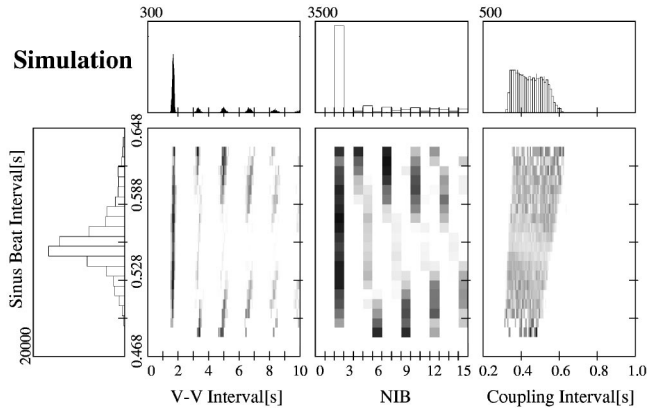

FIG. 11. Simulation of weakly coupled pacemakers based on the sinus beats of Record 3 and the coupling shown in Fig. 10(a). Some noise ($\sigma=0.07$ s) is added to the timings of the ventricular pacemaker and the sinus beat intervals of Record 3 are used in the simulation. Comparison with Fig. 2(c) shows that the simulation reproduces most of the patterns of Record 3. The coupling reduces the number of ventricular beats that are generated. The narrow peak in the coupling interval is not reproduced.

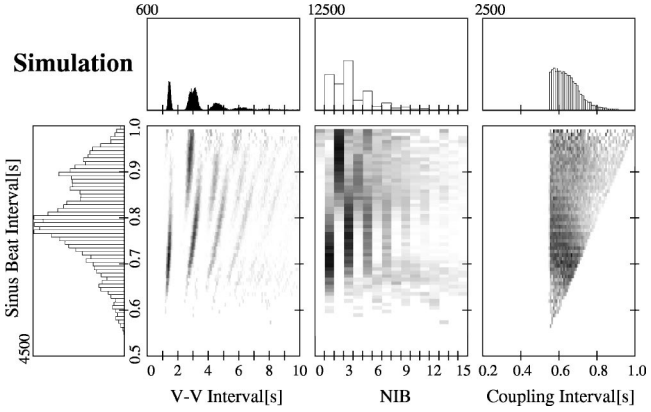

FIG. 12. Simulation of a model with strongly coupled pacemakers with the sinus beat intervals of Record 4. Gaussian distributed noise with a standard deviation $\sigma=0.1$ s was added to the period of the V beats ($T_V=1.50$ s). The refractory time is $\theta=0.55$ s. The coupling is shown in Fig. 10(c).

model are ''missing'' in the data. The reason for these discrepancies may be the coupling between the sinus pacemaker and the ectopic pacemaker [26]. We will therefore continue to discuss this record in the following section as an example of weakly coupled parasystole.

VII. MODEL 3B: COUPLED PACEMAKER—MODULATED PARASYSTOLE

An extension of the third model assumes that the sinus rhythm resets or modulates [27] the ectopic pacemaker in the ventricles [5,8,28]. This interaction can be formulated as a phase resetting curve (Fig. 10), which gives the change of the period of the extra pacemaker as a function of the timing of an intervening sinus beat. A sinus beat appearing in the first part of the ventricular cycle either has no effect or prolongs it. In contrast, a sinus beat appearing in the second part of the ventricular cycle shortens the cycle [5,8,27]. This second part may extend over most of the range.

A system of coupled pacemakers can be described by a difference equation [29]. In its most general form there will also be stochastic fluctuations on the timings of the V beats,

$$\phi_{i+1}=\left(\phi_i+\frac{T_V}{T_S}+\frac{f(\phi_i,T_S,T_V)}{T_S}+\frac{\eta}{T_S}\right) \mod 1, \quad (8)$$

where η is a Gaussian random variable distributed around 0, and $f(\phi_i,T_S,T_V)$ gives the iteratively added change of T_V due to the coupling of the normal beats to the V beats [5,8].

Comparison with Record 3. In Record 3 in Fig. 2(c) the basic features of parasystole are preserved. In a recent study [17], we used the coupling shown in Fig. 10(a) to simulate this heartprint using the sinus beats of the actual data. The result is shown in Fig. 11. Since the coupling shortens T_V only by 7.6%, the basic structure of parasystole is present: equidistant V-V intervals, the NIB triplets, and uniform distribution of the coupling intervals. The coupling leads, for $T_V/T_S\approx 3$, to a fixed point in Eq. (8), such that the V beats always fall in the refractory period of the normal beat and thus are always blocked [30]. In combination with the noise that moves the V beats randomly in and out of the refractory time, the blocking mechanism gives rise to a discrete Poisson process leading to an approximately exponential falloff of the peak heights of the NIB values 2,5,8, . . . [9,31]. Finally, the model gives an accurate estimate of the fraction of V beats as a function of T_S shown in Fig. 3(b).

For other interactions all resemblance to parasystole may be lost. In Fig. 4(d) we present the heartprint of a simulation of two strongly coupled pacemakers using the same system as for the two uncoupled pacemakers in Fig. 4(c). The phase response curve of the coupling is shown in Fig. 10(b), it shortens the time remaining until the next V beat by up to 60%. The peaks in the V-V interval histogram are not equidistant, and the V-V intervals show the diagonal line structure we have seen before. Some structure is still present in the gray scale plot of the NIB but does not correspond to the triplets. The uniform distribution of the coupling intervals is replaced by a strongly peaked one which is more similar to the fixed delay simulation than to the uncoupled pacemakers. In this case it is difficult to recognize parasystole at all and will be even more difficult in the presence of noise on both mechanisms. In general, for a strong coupling, the distinction between coupled parasystole and a mechanism with fixed delay is very difficult, since the coupling leads to phase locking which is effectively a fixed delay.

Comparison with Record 4. The heartprint of Record 4 is shown in Fig. 2(d). Since the coupling intervals cover a broad range, a parasystolic mechanism seems possible. However, in contrast to Record 3, in which the V-V intervals are multiples of a common divisor, the V-V intervals of Record 4 are more widely dispersed. Therefore, if the underlying mechanism is parasystole, resetting must play an important role. This is also evident when comparing the NIB triplets of the data to those for uncoupled parasystole in Fig. 9, where the leftmost dashed arrow indicates the range of this record.

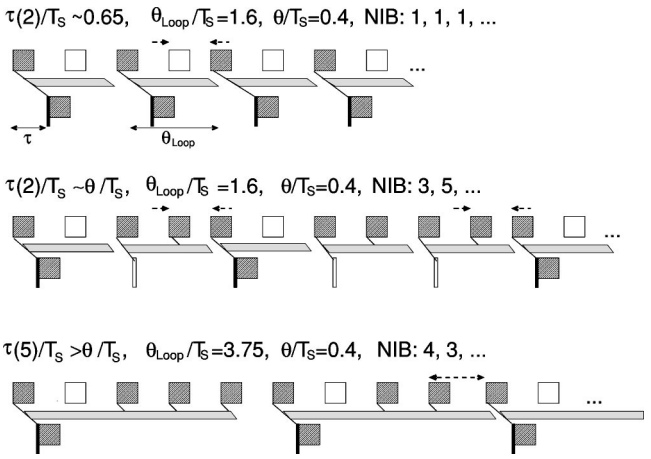

FIG. 13. Schematic plot of a reentry model including a variable refractory time for the reentry pathway.

We estimate $T_V \approx 1.5$ s, and $\theta \approx 0.55$ s from the shortest *V*-*V* and CI interval, respectively. We carried out simulations using various resetting functions. We were able to find agreement with some aspects of the data. Figure 12 shows the results using the resetting curve Fig. 10(c). In the simulation, there is a broad region of concealed bigeminy, NIB $=1,3,5,7,\ldots$ for $T_S = T_V/2 \approx 0.8$ s. In contrast, in Record 4 there is, for $T_S \approx 0.8$ s, a strong presence of NIB$=1$, and 3 only. Although there are qualitative similarities in the gray scale plots of the *V*-*V* and CI intervals, there is only partial agreement with the NIB gray scale plot. We think the underlying mechanism is not clear—and may not be parasystolic.

VIII. DISCUSSION

Reduced to the most basic terms, cardiac rhythms arise from a small number of fundamental processes involving pacemakers and waves of activation (depolarization) and recovery (repolarization). The waves can propagate or they can be blocked. If the waves propagate, characteristics of the propagation such as the duration of the action potential and the velocity of the propagation usually depend on the physiological state of the system. All this activity takes place in an anatomically complex structure.

Given these straightforward theoretical concepts and the importance of cardiac arrhythmia for human health, it is perhaps surprising that our understanding of cardiac arrhythmias is not more advanced. Certainly, some of the striking patterns that we have described are apparent on even the most superficial examination of the electrocardiogram, and have been the subject of clinical description, classification, and theoretical modeling for almost a hundred years. A problem is that different theoretical models can account for the same electrocardiographic pattern. For example, a bigeminal rhythm in which sinus beats and ectopic beats alternate can be accounted for by reentry [32], modulated parasystole [5,6,8], or by triggered automaticity [2]. Consequently, showing agreement between a short stretch of an electrocardiographic record and a given model does not constitute a sharp test of a theoretical mechanism. Computer analyses carried out over longer time intervals are essential for a critical test of any hypothesized mechanism.

Only a few previous studies have considered in detail the dynamical features of complex arrhythmia as provided by 24 h electrocardiographic Holter tape recordings [11,13,14,26]. The important feature of the current work is the comparison of the simulated dynamics (using a hypothesized theoretical mechanism) with the observed dynamics over long times. In developing the theoretical models, we focus on observable features of the dynamics to give insight into the underlying mechanisms. Ectopic beats are only observed during time intervals during which the heart is excitable. Consequently, the gray scale (heartprint) plots of the coupling intervals as a function of the sinus rate, gives information about the refractory period of the heart. If the coupling interval varies widely, this is an indication of a lack of tight coupling between the sinus beat and the ectopic beat as was found in Figs. 2(c) and 2(d). In contrast, if the coupling interval is confined to a narrow range as in Fig. 2(b), this indicates that there is a strong interaction between the sinus beat and the generation of the ectopic beat. In most cases, as a consequence of the refractory time, there are elevated densities along the diagonals in the gray scale plots of the *V*-*V* intervals as a function of the sinus cycle length, Figs. 2(a), 2(b), and 2(d). An exception occurs when the ectopic beats are associated with an independent parasystolic pacemaker, Fig. 2(c), leading to vertical lines in the gray scale plots of the *V*-*V* intervals as a function of the sinus cycle length and sharp peaks separated by multiples of a common divisor in the histogram of the *V*-*V* intervals. Striking regularities in the distribution of the number of sinus beats intervening two ectopic beats are evident in Figs. 2(b), 2(c), and 2(d), but only for Fig. 2(c) was it possible to develop a convincing theoretical interpretation.

We believe that our difficulties in replicating the dynamics of some of the records, especially Record 2, Fig. 2(b), reflect fundamental deficiencies in our understanding of basic underlying mechanisms. We believe that in order to help determine the underlying mechanism in this and other subjects, it might be useful to combine the analysis of the long term electrocardiographic tapes with direct investigations that are possible in subjects who are undergoing clinical electrophysiological studies that enable stimulation and recording directly from the patient's heart.

The current work demonstrates that complex arrhythmia in human hearts recorded over long times displays a number of dynamic features. Appreciation of these features is possible using computer aided analysis of data recorded over long times. Better understanding of the underlying mechanisms of these rhythms should facilitate the development of theoretical models. However, at the present time, it is clear that one model does not fit all—each of the cases we have studied has unique distinguishing features. Developing a better classification of the mechanisms underlying the complex rhythms should be possible, but such efforts will necessarily involve extensive data analysis, physiological insight, and simulation of nonlinear equations.

ACKNOWLEDGMENTS

We thank R. Goldsmith for providing some of the data, and the German Academic Exchange Service (DAAD), NIH/NCRR (Grant No. P41RR13622), NASA, the Mathers Charitable Foundation, and the Canadian Institute for Health Research for support.

APPENDIX: MODEL FOR REENTRY

Figure 13 shows a schematic plot for the beat sequence in a model for reentry. The boxes represent the sinus beats with their refractory time (empty boxes indicate blocked sinus beats), the black bars are the *V* beats (empty bars indicate locked *V* beats). Here every *V* beat blocks the following sinus beat even if it is an interpolated beat. Fluctuations in the otherwise constant sinus beat intervals are indicated by the dashed arrow above. Without fluctuations this model generates stable beat sequences. A sinus beat can start an excitation traveling through the reentry loop, indicated by the diagonal line. The travel time τ through the reentry loop is the horizontal projection of this diagonal line. If it ends after the refractory time of the sinus beat, a *V* beat is generated (black bar). The travel time depends on the recovery time (numbers given in units of T_S), the time elapsed since the last excitation entered the loop. The travel time is shorter if the recovery was longer. After an excitation travels through the loop, no matter if it results in a *V* beat or not, the reentry loop will be refractory for a time θ_{Loop} indicated by the gray narrow trapezoid. During this time no excitation can propagate through the reentry loop. The upper panel the of Fig. 13 indicates that travel time $\tau(2T_S)$ is much longer than the refractory time θ, such that all propagations through the loop result in a *V* beat. The travel time is longer if a shorter sinus beat interval prolongs the recovery time (dashed arrow). In the present case the travel time is still longer than the refractory time and the beat sequence is unchanged. The middle panel of Fig. 13 indicates that the travel time τ is almost the same as the refractory time θ, i.e., for a recovery time of $2T_S$ with the present sinus beat interval T_S the travel time is shorter than the refractory time. Only if a shorter sinus beat interval occurs, the travel time becomes long enough to result in a *V* beat. Thus, if the travel time is of the duration of the refractory time, fluctuations of the sinus beat intervals change the beat sequence significantly. The resulting NIB sequence here consists of the values 1,3,5, . . . , a pattern called concealed bigeminy. The lower panel of Fig. 13 indicates that in the upper and middle panel the refractory time of the reentry loop is too short to play any role. In this case the very long refractory time of the reentry loop dominates the beat sequence. The excitation of only every fourth sinus beat can enter the reentry loop. In the presence of fluctuations, also the third sinus beat may also generate a *V* beat.

[1] E. N. Prystowsky and G. J. Klein, *Cardiac Arrhythmias: An Integrated Approach for the Clinician* (McGraw-Hill, New York, 1994).

[2] P. F. Cranefield, *The Conduction of the Cardiac Impulse: The Slow Response and Cardiac Arrhythmias* (Futura Publishing Co., Mount Kisco, NY, 1975).

[3] Multicenter Post-infarction Research Group, N. Engl. J. Med. **309**, 331 (1983); J. Mukharji, *et al.*, Am. J. Cardiol. **54**, 31 (1984); J.T. Bigger Jr., J.L. Fleiss, R. Kleiger, J.P. Miller, and L.M. Rolnitzky, Circulation **69**, 250 (1984).

[4] The Cardiac Arrhythmia Suppression Trial (CAST) Investigators, N. Engl. J. Med. **321**, 406 (1989); D.S. Echt, P.R. Liebson, B. Mitchell, R.W. Peters, D. Obias-Manno, A.H. Barker, D. Arensberg, A. Baker, L. Friedman, H.L. Greene, M.L. Huther, and D.W. Richardson, *ibid.* **324**, 781 (1991); The Cardiac Arrhythmia Suppression Trial (CAST) Investigators, *ibid.* **327**, 227 (1992).

[5] G.K. Moe, J.J. Jalife, W.J. Mueller, and B. Moe, Circulation **56**, 968 (1977).

[6] M. Courtemanche, L. Glass, M.D. Rosengarten, and A.L. Goldberger, Am. J. Physiol. **257**, H693 (1989); M. Courtemanche, L. Glass, J. Bélair, D. Scagliotti, and D. Gordon, Physica D **40**, 299 (1989); M. Courtemanche, L. Glass, and M.D. Rosengarten, Ann. N.Y. Acad. Sci. **591**, 178 (1990).

[7] N. Ikeda, S. Yoshizawa, and T. Sato, J. Theor. Biol. **103**, 439 (1983).

[8] J. Jalife, Ch. Antzelevitch, and G.K. Moe, PACE **5**, 911 (1982).

[9] L. Glass, A.L. Goldberger, and J. Bélair, Am. J. Physiol. **251**, H841 (1986); L. Glass, A.L. Goldberger, M. Courtemanche, and A. Shrier, Proc. R. Soc. London, Ser. A **413**, 9 (1987).

[10] S. Kinoshita, G. Konishi, M. Sakurai, and S. Ogawa, J. Electrocardiol. **28**, 69 (1995).

[11] R. De Paola, H.-X. Wang, and W.I. Norwood, Am. J. Physiol. **265**, H1603 (1993); H.-X. Wang, R. De Paola, and W.I. Norwood, Phys. Rev. Lett. **70**, 3671 (1993); **71**, 3039 (1993).

[12] K. Takayanagi, K. Tanaka, H. Kamishirado, Y. Sakai, T. Fujito, T. Inoue, T. Hayashi, S. Morooka, and N. Ikeda, J. Cardiovasc. Electrophysiol. **11**, 168 (2000).

[13] D. Sapoznikov and M.H. Luria, J. Electrocardiol. **34**, 225 (2001).

[14] L.S. Liebovitch, A.T. Todorov, M. Zochowski, D. Scheuerle, L. Colgin, M.A. Woods, K.A. Ellenbogen, J.K. Heere, and R.C. Bernstein, Phys. Rev. E **59**, 3312 (1999).

[15] K.M. Stein and P. Klingfield, J. Electrocardiol. **23**, S82 (1990).

[16] A. Babloyantz and P. Maurer, Phys. Lett. A **221**, 43 (1996).

[17] V. Schulte-Frohlinde, Y. Ashkenazy, P.Ch. Ivanov, L. Glass, A.L. Goldberger, and H.E. Stanley, Phys. Rev. Lett. **87**, 068104 (2001).

[18] C.-K. Peng, S. Havlin, H.E. Stanley, and A. Goldberger, Chaos **5**, 82 (1995).

[19] P.Ch. Ivanov, L.A.N. Amaral, A.L. Goldberger, and H.E. Stanley, Europhys. Lett. **43**, 363 (1998).

[20] R.M. Berne and M.N. Levy, *Cardiovascular Physiology*, 6th ed. (C.V. Mosby, St. Louis, 1996).

[21] The sinus beat interval is computed from the average of four consecutive sinus beats where concealed sinus beats are in-

cluded. Since not all sinus beat intervals are equally probable, we normalized each line in each of the gray scale plots by dividing by the corresponding value in the sinus beat interval histogram. In constructing the gray scale plots, we collect all episodes with the same sinus beat interval independent of the time of day at which they occur. For long sinus beat intervals, both in the clinical records and in the models to follow, it often happens that the sinus beat following an ectopic beat is not blocked. Such beats are called interpolated sinus beats. When counting the numbers of sinus beats between ectopic beats, we do not include the interpolated beats in this count.

[22] Numerical simulations of the models are carried out for each mechanism with sinus cycle lengths from 0.5 s to 1.25 s. Each sinus cycle length is simulated for 1000 beats and then increased by $1/128 = 0.007\,812\,5$ s, the typical resolution of clinical records. This amounts to 96 000 sinus beats, which span a time period of 83 625 s (that is almost 86 400 s $= 24$ h). As refractory time we choose $\theta = 0.4$ s, a value typically found in clinical data.

[23] To realize a random distribution of *V* beats we choose equally distributed random numbers between 0 and 1, sort them, and then multiply them with the length of the time period under consideration (86 400 s $= 24$ h). We choose to have a probability of *V* beats of 0.5 per second, and therefore we generate $N = 43\,200$ *V* beats.

[24] A similar function was introduced to explain a phenomenon called AV block in which the passage from the upper chambers to the lower chambers is slowed down in dependence on the time that has elapsed since the last beat.

[25] This ratio is similar to the ratio of expressed ectopic or expressed sinus beats which can be derived from a Farey construction: H.-X. Wang, R. De Paola, and W.I. Norwood, Phys. Rev. Lett. **70**, 3671 (1993).

[26] Y. Murakawa, H. Inoue, T. Koide, A. Nozaki, and T. Sugimoto, Br. Heart J. **68**, 589 (1992).

[27] In the clinical literature such a coupling effect is referred to as modulated or irregular parasystole.

[28] S. Kinoshita, F. Okada, and G. Konishi, Am. Heart J. **124**, 816 (1992).

[29] L. Glass, C. Graves, G.A. Petrillo, and M.C. Mackey, J. Theor. Biol. **86**, 455 (1980); A. Lasota and M.C. Mackey, *Chaos, Fractals and Noise: Stochastic Aspects of Dynamics* (Springer-Verlag, New York, 1994).

[30] Some other coupling curves are possible and yield similar agreement with the data. The coupling curves with the best fit to the data all have a flat or positive first part ($T_V/T_S \leqslant 0.5$) and a negative second part ($T_V/T_S \geqslant 0.5$). This form is similar to physiologically motivated phase resetting curves [5,8].

[31] A. Longtin, Chaos **5**, 209 (1995).

[32] V. Santinelli, M. De Paola, D. Smimmo, P. Turco, and M. Condorelli, Clin. Cardiol. **10**, 49 (1987); S. Kinoshita, G. Konishi, and F. Okada, Cardiol. **81**, 100 (1992).